The Journal of Experimental Biology 202, 321–331 (1999)
Printed in Great Britain © The Company of Biologists Limited 1999
JEB2529

THE INFLUENCE OF TEMPERATURE ON POWER PRODUCTION DURING SWIMMING

I. *IN VIVO* LENGTH CHANGE AND STIMULATION PATTERN

DOUGLAS M. SWANK[1,3,4,*] AND LAWRENCE C. ROME[2,3,4,‡]

[1]*Department of Physiology and* [2]*Department of Biology, University of Pennsylvania, Philadelphia, PA 19104, USA,* [3]*Marine Biological Laboratories, Woods Hole, MA 02543, USA* and [4]*Coastal Research Center, Woods Hole Oceanographic Institution, Woods Hole, MA 02543, USA*

*Present address: Department of Biology, San Diego State University, San Diego, CA 92182, USA
‡Author for correspondence (e-mail: lrome@mail.sas.upenn.edu)

Accepted 14 September; published on WWW 22 December 1999

Summary

Ectothermal animals are able to locomote effectively over a wide range of temperatures despite low temperature reducing the power output of their muscles. It has been suggested that animals recruit more muscle fibres and faster fibre types to compensate for the reduced power output at low temperature, but it is not known how much low temperature actually reduces power output *in vivo*. 'Optimized' work-loop measurements, which are thought to approximate muscle function *in vivo*, give a Q_{10} of approximately 2.3 for power output of scup (*Stenotomus chrysops*) red muscle between 10 °C and 20 °C. However, because of the slower muscle relaxation rate at low temperatures, 'optimizing' work loops requires stimulation duration to be reduced and oscillation frequency to be decreased to obtain maximal power output. Previous fish swimming experiments suggest that similar optimization may not occur *in vivo*, and this may have substantial consequences in terms of muscle power generation and swimming at low temperatures.

To assess more precisely the effects of temperature on muscle performance and swimming, in the present study, we measured the length change, stimulation duration and stimulus phase of red muscle at various positions along scup swimming at several speeds at 10 °C and 20 °C. In a companion study, we determined the effects of temperature on *in vivo* power generation by driving muscle fibre bundles through these *in vivo* length changes and stimulation conditions, and measuring the resulting power output. The most significant finding from the present study is that, despite large differences in the *in vivo* parameters along the length of the fish (a decrease in stimulus duration, an increase in strain and a negative shift in phase) moving posteriorly, these parameters do not change with temperature. Thus, although the nervous system of fish could, in theory, compensate for slow muscle relaxation by greatly reducing muscle stimulation duration at low temperatures, it does not. This lack of compensation to low temperatures might reflect a potential limitation in neural control.

Key words: muscle function, fish, swimming, scup, mechanical power, temperature effect, *Stenotomus chrysops.*

Introduction

Temperature has a large effect on the mechanical power output of muscle. Nonetheless, ectothermal animals appear to locomote in a kinematically similar fashion at different temperatures (Rome, 1982, 1990). In fish, where this has been studied most thoroughly, the power required for swimming is nearly independent of temperature, and it has therefore been proposed that at low temperatures more muscle fibres must be recruited at a given speed (Rome et al., 1984). This theory has been termed the 'compression of the recruitment order theory' (Rome, 1986, 1990). A quantitative analysis of how many additional fibres must be recruited to swim at a given speed at low temperatures has been made on the basis of the changes in the steady-state force–velocity relationship and maximal shortening velocity (V_{max}) with temperature. This analysis suggests that the proportion of additional fibres required at low temperatures would simply be equal to the reciprocal of the Q_{10} for force generation at the appropriate *in vivo* velocity on the force–velocity curve (Rome and Sosnicki, 1990; Rome et al., 1990, 1992b). Recent insights into the importance of the rate of muscle relaxation to power production (Marsh, 1990; Woledge, 1992; Josephson, 1993), combined with the fact that temperature has a very large effect on muscle relaxation rate (Rome and Sosnicki, 1990; Rall and Woledge, 1990; Johnson and Johnston, 1991; Rome et al., 1992b; Swoap et al., 1993; Olson and Marsh, 1993), however, brings into question quantitative descriptions based solely on

temperature effects on steady-state muscle mechanical properties.

It has been suggested that oscillatory power measurements (work loops) may provide a more accurate way to measure muscle power production during locomotion. However, the Q_{10} for power output during *optimized* work loops can be misleading as well. First, *different* oscillation frequencies are optimal for power production at different temperatures, whereas animals use the *same* frequencies to locomote at a given speed at different temperatures (Rome et al., 1990, 1992a). For example, Rome and Swank (1992) found that the Q_{10} for power production during *optimized* work loops of scup muscle is 2.3 between 10 and 20 °C, but this value involved comparing the 20 °C muscle at an oscillation frequency of 5 Hz with the 10 °C muscle at 2.5 Hz. When measured *at a given oscillation frequency*, the Q_{10} ranges from approximately 1 at 1 Hz to approximately 5 at 7.5 Hz and continues to increase with increasing oscillation frequencies. These values might still underestimate the Q_{10} for power production *in vivo* because, in these isolated muscle mechanics experiments, stimulus duration was optimized (i.e. made much shorter at 10 °C) to maximize power production at a given frequency. By contrast, during swimming, there is evidence to suggest that the stimulus duration [i.e. electromyogram (EMG) duration] is the same at both temperatures (Rome and Swank, 1992). At low temperature, these long stimulus durations found *in vivo* would be expected to reduce power production even further below the value measured under optimized conditions at a given frequency (Rome and Swank, 1992).

Thus, these factors conspire to lower dramatically the power output at cold temperatures. This was illustrated in a first attempt to drive muscles under their *in vivo* conditions at cold temperatures. Rome and Swank (1992) found that, at 20 °C, scup red muscles could generate *maximal* power at *in vivo* length change, stimulation duration and oscillation frequency. In contrast, under similar *in vivo* conditions at 10 °C, the muscle could generate only 20 % of the maximal power of which it is capable at that temperature. Interpretation of these experiments was limited because they examined this relationship at only one position on the fish's body. It is now recognized that the length change and stimulation pattern that muscle undergoes during swimming varies along the length of the fish (van Leeuwen et al., 1990; Rome et al., 1993; Jayne and Lauder, 1995b; Hammond et al., 1998), as do the mechanical properties of the muscle (Rome et al., 1993; Altringham et al., 1993; Davies and Johnston, 1995; Swank et al., 1997). Thus, although little power is generated in certain regions of fish at cold temperatures, other regions may have closer to optimal length change and stimulation conditions (e.g. a shorter stimulation duty cycle) and more advantageous contractile properties (e.g. faster relaxation) for power generation at low temperatures.

The goal of the overall project was to investigate the temperature effects on muscle power production during *in vivo* stimulation and length-change conditions, so we can better understand how the red muscle of fish provides power for swimming at different temperatures. In this first report, we examine temperature effects on *in vivo* strain, stimulus duration and stimulus phase of the red muscle during swimming. In a companion report (Rome et al., 1999), we examine how temperature affects muscles working under these *in vivo* conditions.

Materials and methods

The main experimental goal of this study was to determine the length change and stimulation patterns the muscle undergoes during swimming so that they could be subsequently imposed on isolated muscles (as in Rome et al., 1993). This required the development of a number of specialized techniques. Many of these techniques are described only briefly in Rome et al. (1993), so they are described in more detail here.

Fish

Scup (*Stenotomus chrysops* L.) 20–25 cm in total length were caught by hook and line in Woods Hole, MA, USA, and were housed in fibreglass tanks through which fresh 20 °C sea water flowed for at least 6 weeks prior to experimentation. Before experimentation at 10 °C, the flow rate of salt water was decreased and the temperature was maintained at 10 °C by a compressor for 24 h. Hence, these experiments were designed to measure acute effects of temperature on 20 °C-acclimated fish. The fish were fed squid, clams and commercial food pellets every other day and kept on a 14 h:10 h light:dark photoperiod.

Anaesthesia

Fish were anaesthetized by perfusing their gills with 50 mg l^{-1} tricaine methanesulphonate (MS222) during the surgical procedures. Following the surgical procedures, the fish were placed in individual holding tanks to recover. During the initial phase of recovery, the fish were moved by hand around the tank to ventilate their gills.

Electromyography

Electromyograms (EMGs) were recorded from the red muscle at four positions along the length of the fish (ANT-1, ANT-2, MID and POST; 29 %, 40 %, 54 % and 70 %, respectively, down the length of the fish). The initial positioning of the electrodes was accomplished by photoreducing a template of a scup to the appropriate length and using this as a guide for electrode placement. To increase the probability that all four electrodes were successfully positioned in the red muscle, a line centred over the red muscle was drawn horizontally on the fish. At each position, scales were removed above the red muscle to form an entry path for a hypodermic needle holding a pair of electrodes (Rome et al., 1992a). The vertical distance between the entry point and the red muscle line was marked on the shaft of the hypodermic needle, and the needles were inserted only to that point.

EMGs were also recorded from the white muscle at a

position corresponding to the ANT-2 position. The white muscle electrodes were placed approximately half-way between the red muscle and the fish's dorsal aspect in the dorsal–ventral plane and centred in the white muscle in the medial plane. Each of the five electrode pairs was sutured to the skin adjacent to the entry point with some strain relief. The electrodes were also run through tack points along the dorsal aspect of the fish's body and sutured together at the front of the first dorsal spine. To prevent tangling prior to experimentation, the electrode wires were ensheathed in spirally split plastic tubing, which was subsequently coiled. During the swimming experiments, the plastic tubing was removed.

EMGs were recorded using Grass P511 preamplifiers fitted with high-impedance probes. Amplifications of 10 000–50 000-fold were used, and channels were typically filtered below 60 Hz and above 3 kHz (Rome et al., 1992a). Each channel was recorded at 5 kHz with a computer-based A/D system (Datapac by Run Technology) on a 486 computer. Although considerable effort was expended on shielding and grounding (i.e. the swimming tube was encased by a Faraday case), we still recorded very brief spikes (approximately 10 μs) coming from the motor controller of the flume (Rome et al., 1992a). The spikes occupied only one data point, leaving the preceding and subsequent points unaffected. Normal (low-pass) analog pre-sampling filtering or digital post-sampling filtering techniques removed the spikes, but they caused perturbations in the preceding and subsequent points. Instead, the spikes were removed digitally using a software macro (DATAPAC) by essentially 'drawing a straight' line between the preceding and the subsequent points. The timing of this correction was set by the white muscle channel, whose EMG was recorded in a manner that maximized the spike height (large gain, low-pass filter moved to 10 kHz). This procedure removed the spikes at a 10-fold higher frequency (5000 Hz) than the frequency of the EMG (<500 Hz) and, hence, did not cause any distortion of the signal.

Filming and muscle length changes

Fish were swum in a recirculating water treadmill (as in Rome et al., 1990, 1992a). The diameter of the test section (20 cm) far exceeded the maximum tail-beat amplitude (4 cm) and tail height (5 cm) (Rome et al., 1992a). Thus, it is unlikely that the fish's movements were restricted while swimming in the water treadmill. Fish were filmed from above at 200 frames s^{-1} with a Locam (Redlake) high-speed cine camera fitted with a video viewfinder (as in Rome et al., 1992a). All swimming sequences were simultaneously videotaped to provide immediate feedback about the quality of each film sequence and to provide an accurate record of the experiment. To aid in cross-referencing the video and film, the period during which the cine camera ran was evident on the video tape in two ways: (1) the 'cine camera-on' signal started the video stopwatch (time/date generator) and (2) the cine film frame counter (see below) was activated and was visible on the video tape.

Muscle length changes were determined as the product of curvature of the backbone (Rome and Sosnicki, 1991) and a calibration equation of sarcomere length *versus* backbone curvature and distance from the backbone (Rome et al., 1992a). The magnitude and phase of the strain recordings determined by this 'anatomical-cine' technique are the same as those determined by the independent technique of sonomicrometry (Coughlin et al., 1996).

Electrical and mechanical wave speed

Electrical wave speed is defined as the speed at which the wave front of electrical activity (i.e. the EMG onset time) passes the EMG electrodes situated along the length of the fish. The mechanical wave speed is defined as the speed at which a characteristic of the bending wave (in our case, maximal muscle length) moves past the positions along the length of the fish where muscle length was being measured.

Combining EMG and length changes

To drive the isolated muscles accurately through the measured *in vivo* parameters, it was essential to obtain very accurate synchronization of EMG and length changes. This required the development of specialized techniques.

Temporal synchronization

The first problem was accurate synchronization of the EMGs (continuous) with muscle length changes (frame-based). The problems encountered and the digital synchronization device developed to solve the problems are described elsewhere in detail (Rome, 1995) and are discussed only briefly here. Typical synchronization techniques provide only ±1 film frame resolution (e.g. 5 ms at 200 frames s^{-1}), and this resolution often deteriorates (progressive desynchronization) as the film sequence proceeds. In the long film sequences we used (approximately 5 s), if the camera framing rate varied by only 0.5 % from expected (i.e. 199 *versus* 200 frames s^{-1}), this would lead to a desynchronization of 25 ms by the end of the sequence. In the best case where there is no desynchronization, 10 ms uncertainty (i.e. ±1 frame) represents 23 % uncertainty in the stimulus phase at 6.4 Hz (the mean tail-beat frequency at 80 cm s^{-1}), which can have important effects on the muscle power production. Larger discrepancies caused by progressive desynchronization will result in larger amounts of uncertainty in determination of phase. The digital synchronization device prevented progressive desynchronization and gave resolutions of better than one frame (±0.2 ms) or less than 1 % uncertainty in phase (Rome, 1995).

Measurements of length changes and EMG at the same position on the fish

The electrical wave of excitation and the mechanical wave of bending move down the fish at different speeds (see Results). Accurate determination of the phase of the EMG with respect to muscle length change requires that the muscle length change be measured at the exact position on the fish where the electrodes are placed. This was

accomplished as follows: after each experiment, a stereotaxic device was used to measure the exact position of each electrode along the length of the dead fish held in a straight position. These values were then input into the computer, and a program measured down the length of the backbone (determined from the film after correcting for approximately 4 % parallax error) and located the corresponding point on the fish's curved surface during swimming. We verified that this procedure accurately determines the position of the EMG electrodes (and thus the muscle strain at the position of the electrodes) as the fish went through its oscillatory bending by suturing reflective markers to the electrode positions on the side of the fish and following their movements during swimming.

Determination of time of peak muscle length

Phase is defined as the proportion of the tail-beat cycle (in degrees) by which the onset of the EMG precedes the maximum length of the muscle, and hence the onset of shortening (Rome and Swank, 1992). Determining the precise timing of the maximum muscle length is made difficult because of the discontinuous nature of the muscle length data (frame base) as well as noise in the determination of muscle length change. Although the signal-to-noise ratio was excellent in the POST and MID positions, it became progressively worse moving anteriorly, principally due to shorter strains (see Fig. 2). We used a three-step analysis procedure (using MATLAB by Mathworks) to determine better the timing of muscle length amplitude maxima. First, spectral analysis was performed on the raw data. Second, the data were digitally filtered on the basis of the spectral analysis (see Fig. 2). Finally, a spline routine was used on the filtered data to find the timing of the muscle length maximum. We found that the procedure used to filter the data did not cause any phase shift in the length maxima.

Determination of EMG onset and offset times

Accurate determination of the phase and stimulation duration requires precise measurement of the onset and offset times of EMG activity in each length-change cycle. EMG onset time was determined by eye or by one of two software routines. In both software routines, the EMGs were first rectified. In one routine, a threshold was chosen, while in the other routine the derivative of the rectified trace was obtained and this signal was then thresholded. The advantage of using the derivative is that low-frequency motion artefacts occurring at the end of the EMG burst could be removed (see Fig. 5). In each case, the EMG burst was considered to start on the first spike and end immediately after the last spike that exceeded the threshold. It is recognized that fine distinctions made by various schemes are inherently arbitrary. However, a sensitivity analysis of our muscle mechanics results in Rome et al. (1999) showed that the whole procedure of reproducing in isolated muscle the *in vivo* length change and stimulation pattern was relatively insensitive to which EMG analysis procedure was used.

Experimental protocol

Following implantation, each of the seven animals was swum at 10 °C and 20 °C over the full range of speeds that they could power without recruiting their white muscle, as well as at speeds at which white muscle was initially recruited. At 10 °C, fish were swum from 20 cm s^{-1} to 60 cm s^{-1}. At 20 °C, they were swum from 30 cm s^{-1} to 90 cm s^{-1}. Our goal was to analyze both the slowest speed and the fastest speed at which the fish could swim steadily at each temperature without recruitment of their white muscle. Because of individual variation, to ensure that each fish could swim at the chosen speed, we analyzed swimming speeds of 80 cm s^{-1} (some data reported in Rome et al., 1993) and 50 cm s^{-1} at 20 °C, and at 50 cm s^{-1} and 30 cm s^{-1} at 10 °C. Fish were given 24 h to recover from anaesthesia and 48 h between swimming bouts at different temperatures.

Statistics

Statistical analyses were performed using SigmaStat software (Jandel). To compare means, *t*-tests were typically used, and analysis of variance (ANOVA) was used in some cases. Statistical significance was set at $P<0.05$. Linear regressions were also performed and considered significant if the slope differed from zero at $P<0.05$.

Results

Kinematics and sarcomere length changes during swimming

Tail-beat frequency increased with swimming speed and at some swimming speeds was slightly lower at 10 °C than at 20 °C. This difference, although significant, is quite small (Fig. 1A). Previous findings showed that tail-beat frequency at a given speed was essentially independent of temperature (Rome et al., 1992a).

As found previously (Rome et al., 1992a), the strain, and thus the signal-to-noise ratio, was much larger in the posterior of the fish than in the anterior (Figs 2, 3B). In the ANT-1 position, the oscillatory length change pattern was sometimes difficult to discern in the raw data because of the low strain and low signal-to-noise ratio (Fig. 2).

Spectrum analysis of muscle length-change recordings showed a clear peak at the fish's tail-beat frequency. The amplitude of that peak-to-peak excursion increased posteriorly (Fig. 3B). In the MID and POST regions of the fish, spectrum analysis often showed peaks at higher harmonics of the tail-beat frequency. In the ANT-1 and ANT-2 positions, higher harmonics were not consistently apparent.

The strategy for filtering muscle length-change recordings was to provide the most accurate determination of the timing of the maximum length, which was critical for the determination of wave speed and EMG phase, while retaining as much shape information as possible. Therefore, digital filtering (eight-pole Butterworth filter) for ANT-1 and ANT-2 was performed above the first harmonic (amplitude reduced by 50 % at 1.5 times tail-beat frequency); for MID and POST, it was performed above the second harmonic (amplitude reduced

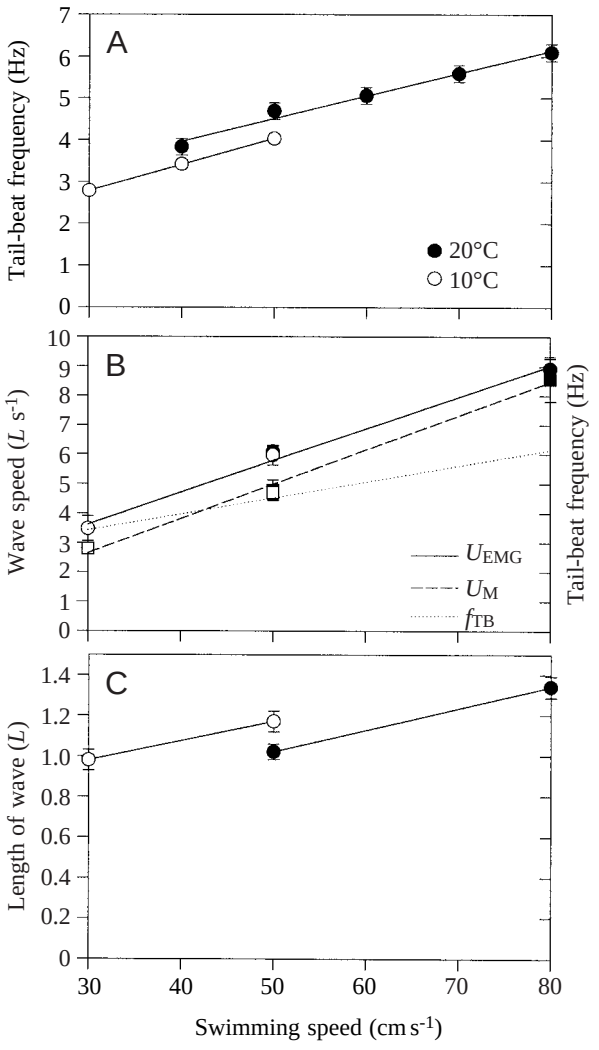

Fig. 1. Tail-beat frequency, mechanical and electrical wave speeds, and length of the bending wave as a function of swimming speed U and temperature. (A) Tail-beat frequency f_{TB} increased with swimming speed U (f_{TB}=0.06U+0.92, r^2=0.99 at 10 °C and f_{TB}=0.054U+1.8, r^2=0.98 at 20 °C) and was slightly slower at 10 °C than at 20 °C for swimming at 50 cm s^{-1} (t-test, P=0.027) but not at 40 cm s^{-1} (t-test, P=0.81). (B) The speed at which the mechanical bending wave (squares, filled at 20 °C, open at 10 °C) and the electrical wave (circles, measured from electromyogram, EMG, onset times) moved along the length of the fish increased linearly with swimming speed. The EMG wave speed U_{EMG} (U_{EMG}=0.108U+0.39, r^2=0.99) was somewhat faster than the mechanical bending wave speed U_M (U_M=0.116U–0.85, r^2=0.99), resulting in more negative phases in the posterior regions of the fish (see Fig. 3). Note that the tail-beat frequency f_{TB} (at 20 °C, dotted line) increased with swimming speed at a slower rate than the mechanical wave speed. This causes an increase in the length of the bending wave (λ_B) on the fish with increasing speed as shown in C (one-way ANOVA, P<0.001). The length of the bending wave during swimming at 50 cm s^{-1} is significantly higher at 10 °C than at 20 °C (t-test, P=0.043). Values are means ± S.E.M. (N=5–7). L, body length.

by 50 % at 2.5 times tail-beat frequency). Filtering out higher harmonics necessarily makes the length changes appear more ‘sinusoidal’ than in the raw recordings. The filtered data (superimposed over the raw data) are shown on the right-hand side of Fig. 2. In each case, the filtering was also performed at one higher harmonic (2.5 times tail-beat frequency for ANT-1 and ANT-2, and 3.5 times tail-beat frequency for MID and POST) to assess whether ‘overfiltering’ was altering the determination of the peak amplitude values.

This analysis showed that the strain recordings were not significantly overfiltered. The raw data from the MID and POST positions were nearly indistinguishable from the filtered data. More anteriorly, the noise in the raw recording increases, and hence the differences between it and the filtered recording become more noticeable. In ANT-2, this discrepancy is small but, as expected, in ANT-1 it became larger.

In the ANT-1 position, the relatively large amplitude of high-frequency noise in the raw recordings gives the appearance that filtering may have reduced our determination of strain. However, Fig. 1 in Coughlin et al. (1996) showed that this same filtering technique has no effect on the amplitude of sonomicrometry recordings (which are inherently less noisy). Further, these authors found that the amplitudes for the ANT-1 derived from *filtered* length recordings based on film analysis agreed very well with amplitudes from *unfiltered* sonomicrometry recordings. This suggests that, even in ANT-1, our filtering scheme effectively removed high-frequency noise and had little effect on amplitude.

It should be noted that with the 2.5 times tail-beat frequency filter, the amplitude of the ANT-1 strain appeared to be 20 % higher than with the 1.5 times tail-beat frequency filter shown in Fig. 2. However, the 2.5 times tail-beat frequency filter was not used, because it did not provide as accurate phase information as the 1.5 times tail-beat frequency filter. By driving muscles under a 25 % larger strain to account for possible over-filtering, we show in a sensitivity analysis in Rome et al. (1999) that this potentially small increase in strain at ANT-1 would have no effect on its power production.

The higher harmonics evident in the MID and POST regions are consistent with the muscle length change having some aspects of a triangular wave, rather than being purely sinusoidal. We found that a triangular wave fitted the data with a slightly better r^2 than did a sinusoid; however, it is difficult to differentiate clearly between these different waveforms statistically. Therefore, in Rome et al. (1999), we used a digitally rounded triangular wave that is intermediate between a sinusoid and triangular wave to represent the length change at the MID and POST positions.

The peak amplitude and the timing of that peak were found by an interpolated spline routine of the filtered data. The strains (presented as ± strain around a central value) became increasingly larger moving from ANT-1 to POST (from approximately ±1.5 % to approximately ±5.5 %) (Fig. 3B). Except for the ANT-1 position, there also appeared to be a small increase of strain with swimming speed (Fig. 4B), as previously found (Rome et al., 1992a). At 50 cm s^{-1}, the strain at 20 °C tended to be slightly longer in POST and MID than at

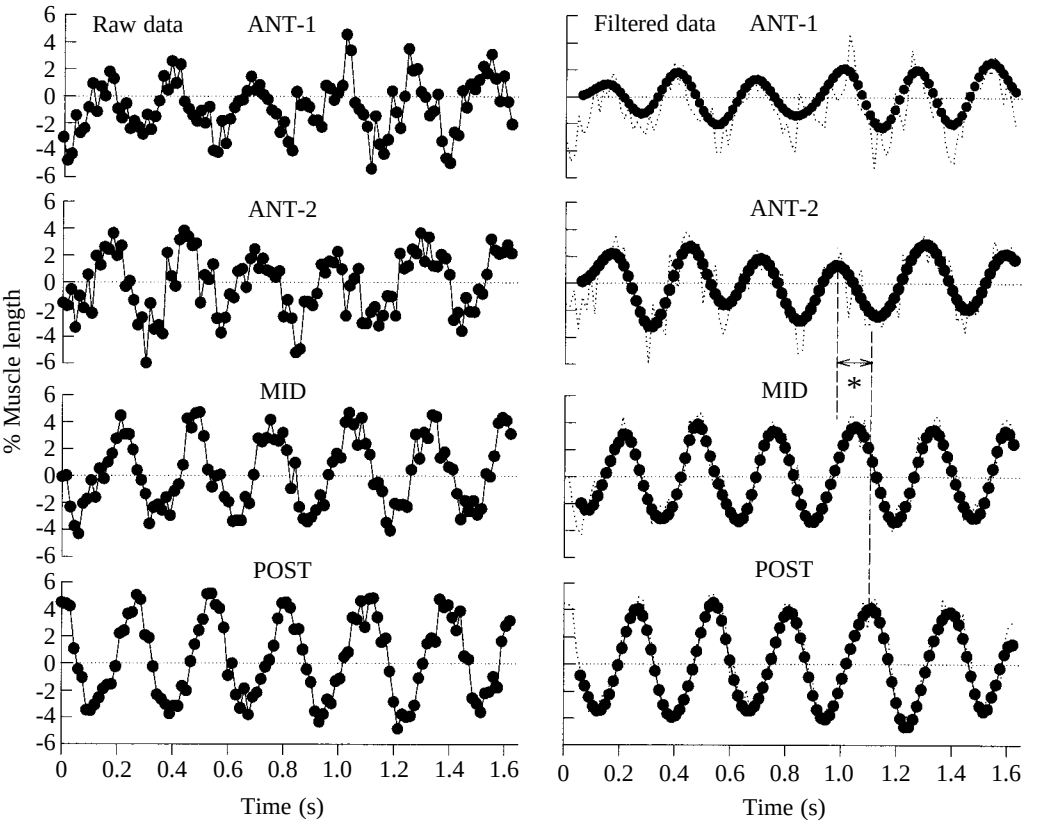

Fig. 2. Typical changes in muscle length at the ANT-1, ANT-2, MID and POST positions for a scup swimming at 30 cm s^{-1} at 10 °C. The left side shows the raw muscle length change data generated by digitizing the outline of the fish from high-speed cine frames. The right side shows the same data after smoothing using an eight-pole Butterworth filter set at 1.5 times tail-beat frequency for ANT-1 and ANT-2, and 2.5 times tail-beat frequency for MID and POST; for comparison, the raw data are also plotted (dotted lines). Note that the strain in the ANT-1 and ANT-2 positions for this fish was somewhat larger than the mean values illustrated in Fig. 3. The speed of the bending wave (U_M) was calculated as the quotient of the time difference (*) of maximum muscle length occurrence at the ANT-2 and POST positions (dashed vertical lines) and the distance between these two positions on the fish.

10 °C; however, these differences were not significant (*t*-tests, *P* ranged from 0.10 to 0.18). The strain amplitude values were somewhat lower than we had reported previously using unfiltered data (Rome et al., 1992a). The raw tracings of Rome et al. (1992a) appear to have less noise than those reported here. In the following paper (Rome et al., 1999), we also measure power production using the strains found in Rome et al. (1992a).

Mechanical wave speeds and wavelength of the bending wave

Mechanical wave speed is the speed at which the bending wave moves along the fish's body (Fig. 1B). Because of the reduced signal-to-noise ratio in the ANT-1 position in some fish, we measured the speed as the bending wave moved from the ANT-2 to the POST positions (Fig. 2). The mechanical wave speed increased in a linear fashion with swimming speed from approximately 2.8 to 8.6 fish lengths s^{-1} (Fig. 1B). At 50 cm s^{-1}, there was no difference in wave speed between fish swimming at 10 °C and 20 °C.

We also determined wavelength of the bending wave (λ_B) at different swimming speeds and temperatures. The wavelength of the bending wave is related to mechanical wave speed (U_M) and tail-beat frequency (f_{TB}) by the equation:

$$\lambda_B = U_M/f_{TB},$$

Fig. 1 shows that although both tail-beat frequency and mechanical wave speed increase linearly with swimming speed, the mechanical wave speed increases with a steeper slope than tail-beat frequency (*t*-test, $P<0.001$). As the ratio of wave speed to tail-beat frequency increases with swimming speed, λ_B should increase as well. We determined λ_B by analyzing the relative phase of the bending wave between the ANT-2 and POST positions on the fish. We found that λ_B determined in this way increases from approximately 0.98*L* at 30 cm s^{-1} to approximately 1.34*L* at 80 cm s^{-1} (*L* is fish length; Fig. 1C). The change in λ_B with swimming speed has been noted previously in bass *Micropterus salmoides* by Jayne and Lauder (1995a).

Electromyography

EMGs were recorded from four positions along the length of the fish and were characterized by a high signal-to-noise ratio (Fig. 5). The EMG data of the ANT-1 and POST positions presented specific analysis problems. First, rather than being fairly constant in magnitude throughout activation, the EMG in the ANT-1 position sometimes started with low-amplitude spiking. We assumed that the EMG commenced with the first spike. However, the uncertainty in when ANT-1 EMGs begin contributes to errors in determining EMG onset time and, hence, EMG duration and phase for this position (see Discussion). Second, at the POST position, the motion artefact was more noticeable than in other regions of the fish, presumably because of the large strain of the muscle and the large lateral displacement of the tail.

EMG duty cycle decreased moving from the anterior of the fish to the posterior positions (Fig. 3A, see also Fig. 6). It

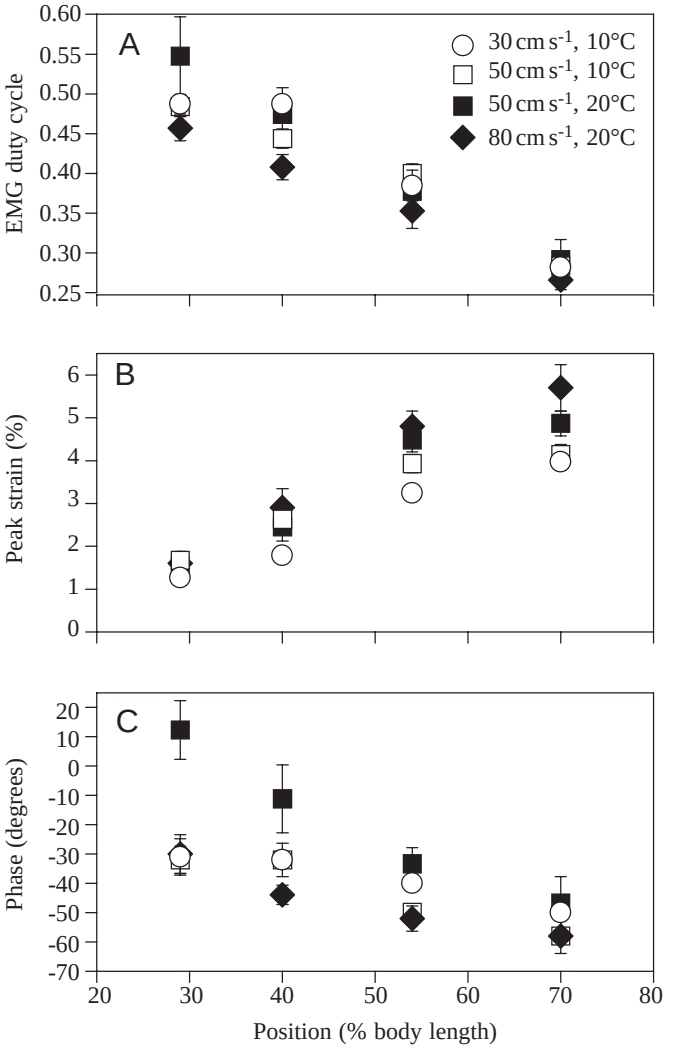

Fig. 3. Electromyogram (EMG) duty cycle, strain and phase as a function of body position, speed and temperature. (A) EMG duty cycle became progressively shorter towards posterior positions at both temperatures. (B) Peak strain was greatest at the POST position (70 % body length *L*) and decreased moving anteriorly. (C) Phase is more negative towards the posterior of the fish (one-way ANOVA; 30 cm s^{-1}, P=0.009; 50 cm s^{-1} 10 °C, P<0.001; 50 cm s^{-1} 20 °C, P=0.003; 80 cm s^{-1}, P=0.007). The anterior positions have larger error bars because of their small strains, which caused difficulty in determining precisely the timing of maximum muscle length. Values are means ± S.E.M. (N=5–7 animals). For each animal under each condition, 4–6 tail beats were analyzed.

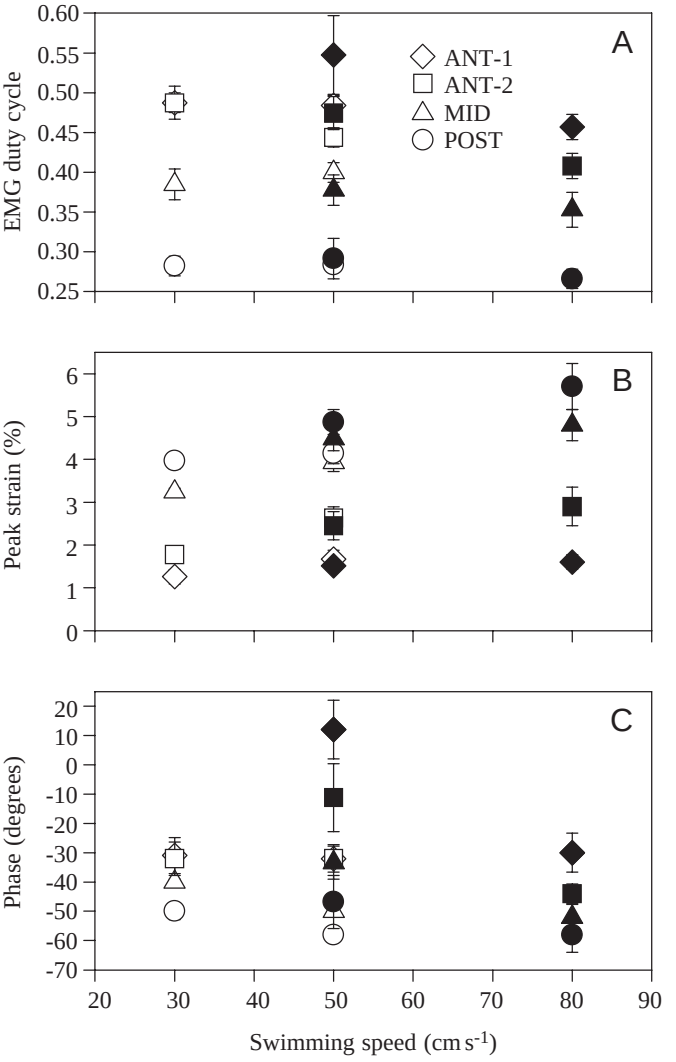

Fig. 4. Electromyogram (EMG) duty cycle, strain and phase as a function of swimming speed, temperature and body position. Filled symbols denote a swimming temperature of 20 °C, open symbols denote 10 °C. (A) Except for the ANT-2 position, EMG duty cycle showed little change with swimming speed (one-way ANOVA: ANT-1, P=0.11; ANT-2, P=0.004; MID, P=0.14; POST, P=0.253). (B) Strain increased slightly with swimming speed at all positions except the ANT-1 position (linear regression: ANT-1, P=0.269; ANT-2, P=0.004; MID, P<0.001; POST, P=0.027). (C) No variation in phase with speed or temperature was observed. The data at 50 cm s^{-1} at 20 °C for ANT-1 and ANT-2 seemed to be divergent from the rest of the measurements (see Discussion). Values are means ± S.E.M. (N=5–7 animals). For each animal under each condition, 4–6 tail beats were analyzed.

dropped from approximately 50 % at the ANT-1 position to approximately 27 % at the POST position. This trend is apparent in the raw EMGs from the four positions of the fish (Fig. 5). In our manual analysis, the EMG duration seemed to be a constant proportion of the tail-beat cycle (constant duty cycle) that changed little with swimming speed and did not change with temperature (Fig. 4A). The only data points that appeared to diverge from this pattern were in the anterior regions at 50 cm s^{-1} at 20 °C, but this was not statistically significant (*t*-tests: ANT-1, P=0.17; ANT-2, P=0.249).

As explained in Rome et al. (1999), the durations measured at 10 °C were longer than was optimal for power production. Hence, it was of interest to determine EMG duration using another set of criteria that might be less sensitive to motion artefacts, and thus might yield shorter EMG duty cycles. Further, because the anterior EMG duty cycle values at 50 cm s^{-1} at 20 °C seemed to diverge from the other data, it was of interest to determine EMG duty cycle over a wider

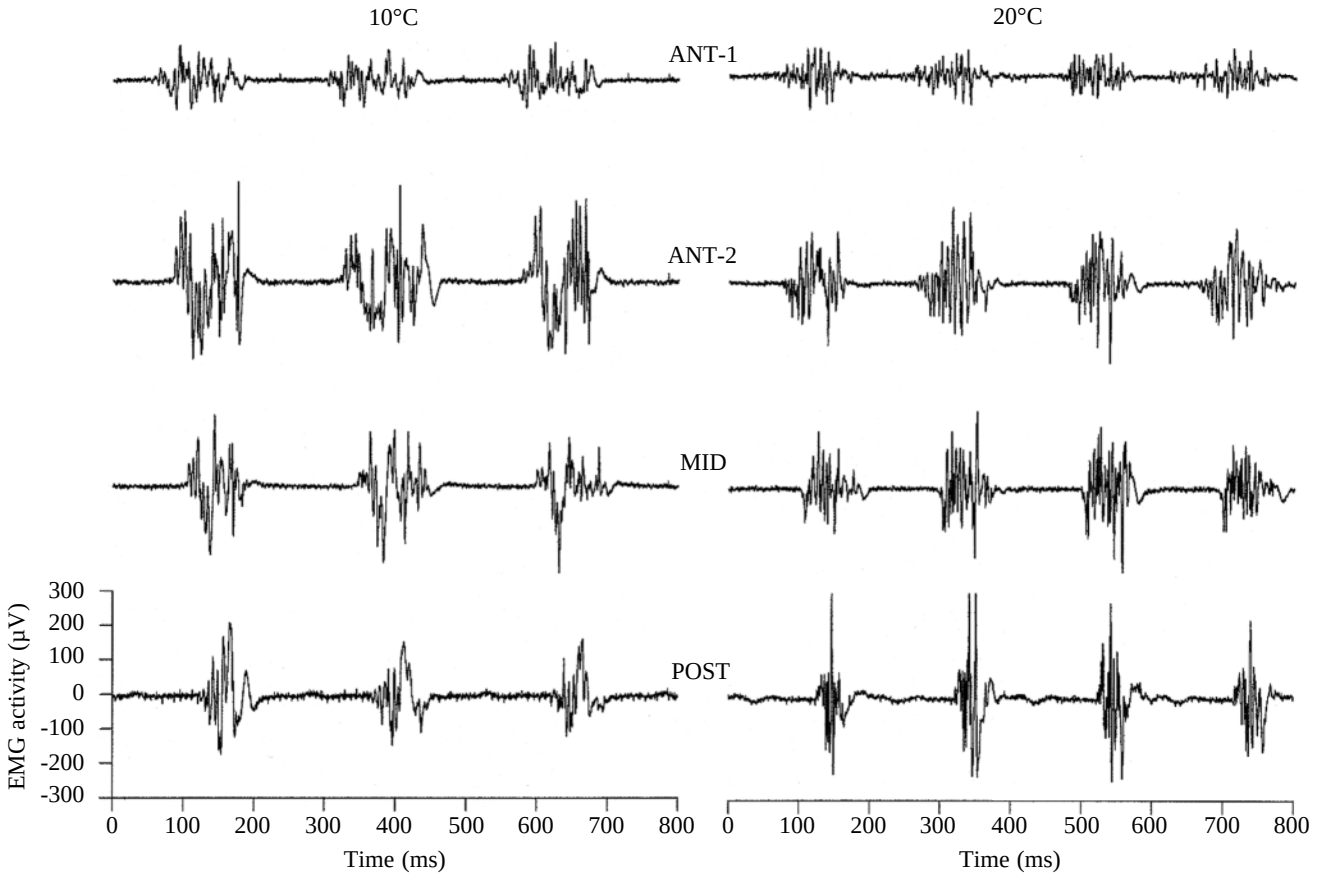

Fig. 5. Typical electromyogram (EMG) traces from a fish swimming at 50 cm s^{-1} at 10 °C and 20 °C. Tail-beat frequency is slightly higher at 20 °C than at 10 °C and, thus, there are more frequent EMG bursts.

range of swimming speeds. We therefore used a custom-designed routine in DATAPAC to rectify the EMGs and then take the derivative of the rectified trace and threshold it. As can be seen in Fig. 6, this procedure reduces the stimulus duty cycle slightly (by approximately 0.05 of a cycle). Using this analysis, there was a small, but significant, decline in EMG duty cycle with increasing swimming speed. However, there was no significant difference between EMG duty cycle at 10 °C and 20 °C.

EMG wave speed versus mechanical wave speed, and the phase of EMG

The EMG wave speed represents the speed at which the EMG onset time moved along the length of the fish. As for the mechanical waves, we measured the average wave speed between the ANT-2 and POST positions. It increased linearly with swimming speed from 3.48 L s^{-1} at 30 cm s^{-1} (10 °C) to 8.92 L s^{-1} at 80 cm s^{-1} (20 °C). Again, at 50 cm s^{-1}, there was no difference in wave speed between fish swimming at 10 °C and 20 °C (Fig. 1B).

As has been generally found in other species, the EMG wave speed was faster than the mechanical wave speed (Williams et al., 1989; van Leeuwen et al., 1990; Wardle and Videler, 1993; Jayne and Lauder, 1995b). In scup, EMG wave speed ranged from 26 % to 30 % faster than mechanical wave speed for fish swimming at 30 cm s^{-1} at 10 °C and at 50 cm s^{-1} at both temperatures (*t*-test, P ranged from 0.006 to 0.019). Although at 80 cm s^{-1}, the EMG wave speed tended to be approximately 9 % faster than the mechanical wave speed, this was not statistically different (*t*-test, P=0.571) (Fig. 1B).

The faster EMG wave speed results in a systematic shift in the start of the EMG signal with respect to muscle shortening. This causes the EMG phase to become more negative (that is the muscle is activated earlier in lengthening) moving from the anterior to the posterior along the length of the fish (Fig. 3C). This shift in phase with position was significant. In general, no difference in phase with temperature or speed was observed (Fig. 4C). Again data at 50 cm s^{-1} at 20 °C in the anterior portion of the fish seemed to diverge from the rest of the measurements (see Discussion).

The length change and stimulation pattern of scup swimming at different speeds and temperatures are summarized in Fig. 7. The data on scup seem to be similar to those of other fish, such as carp and saithe (Wardle et al., 1995).

Recruitment of white muscle

The white muscle is initially recruited at approximately a 1.4-fold higher speed at 20 °C than at 10 °C. The white muscle was initially recruited at 81±0.5 cm s^{-1} (N=7) at 20 °C and at approximately 58±0.4 cm s^{-1} (N=7) at 10 °C. These values

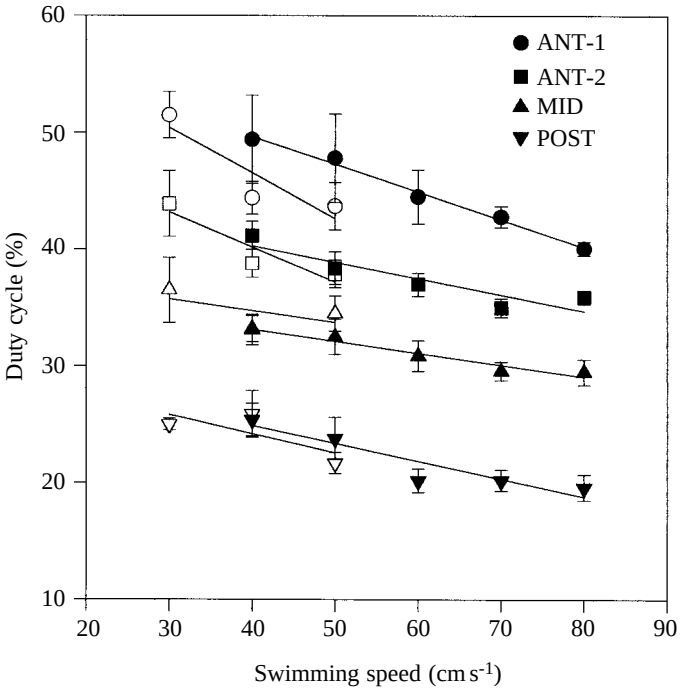

Fig. 6. Computer analysis of electromyogram (EMG) duty cycle as a function of swimming speed, temperature and body position. The method of analysis for this data set differs from that of Fig. 3A and Fig. 4A in that the EMG signal was first rectified, a derivative was taken, and a specific threshold chosen (typically 12 μV) that a software subroutine used to automatically determine the onset and offset times of the EMG burst. Duty cycles were slightly shorter than those determined manually (Fig. 3A) and showed a small decrease with swimming speed at all positions (two-way ANOVA, P=0.009 for 10 °C and P<0.001 for 20 °C). No significant difference was found between 10 °C (open symbols) and 20 °C (filled symbols) (two-way ANOVA, P=0.212 for 40 cm s^{-1}, P=0.367 for 50 cm s^{-1}). Values are means ± S.E.M. (N=5–7 animals). For each animal under each condition, 4–6 tail beats were analyzed.

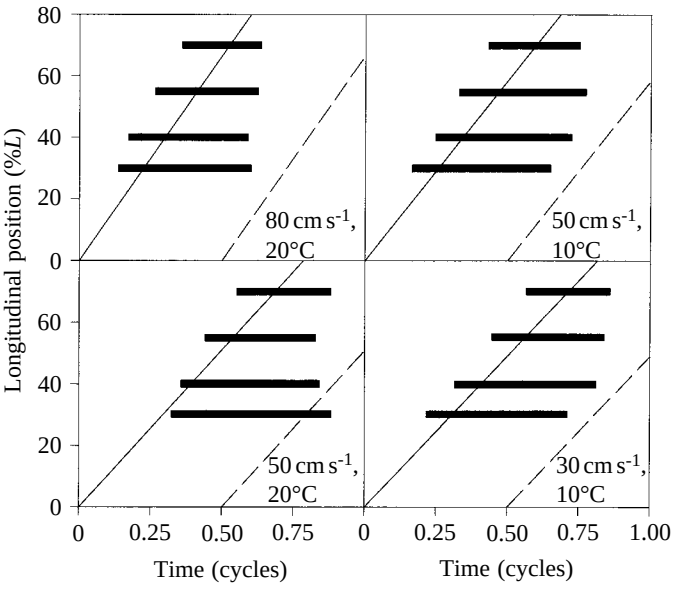

Fig. 7. Electromyogram (EMG) duration and phase as a function of body position under the four swimming conditions. On the basis of the format of Wardle et al. (1995), the horizontal bars represent the time during the tail-beat cycle during which EMGs occur. The position of the bar in the y direction represents the position on the fish. The diagonal solid line represents a phase of zero, i.e. the point of the muscle length maxima. In almost all cases, muscle stimulation starts (left edge of the bar) prior to muscle shortening and ends (right edge of the bar) well before muscle lengthening begins (dashed line). L, fish length.

were very similar to those (54 and 80 cm s^{-1} at 10 and 20 °C, respectively) obtained previously (Rome et al., 1992a).

Discussion

Swimming as a function of speed and temperature: does the nervous system compensate for low temperature?

Rome et al. (1992b) have previously shown that muscle at 10 °C has a 1.6-fold slower V_{max} and takes 2.8-fold longer to relax than at 20 °C. Thus, under *optimized* work-loop conditions, muscle at 10 °C generates 2.3-fold lower power than at 20 °C (Rome and Swank, 1992). It is important to recognize that the use of *optimized* work loops represents the 'best-case' scenario. Because of the slower relaxation rate, not only does low temperature reduce the maximum power muscle can generate, but to generate this maximum power at low temperatures, the muscle at 10 °C must be stimulated with a lower duty cycle and operate at a much lower oscillation frequency than at 20 °C (Rome and Swank, 1992). If the stimulation and length changes are not accordingly adjusted at low temperatures, the power output of the muscle is greatly reduced. For instance, Rome and Swank (1992) found that at an oscillation frequency of 4.5 Hz, when stimulated at a duty cycle appropriate for the ANT-2 position (0.42), the 10 °C muscle generated less than 20 % of the maximum power for 10 °C even with a large strain and optimized phase. In contrast, at 20 °C, the muscle could generate nearly its maximal power under these conditions. Thus, instead of a 2.3-fold difference between 10 °C and 20 °C (found in optimized work loops), there was an approximately 10-fold difference in power generation.

To generate near-optimal power at 10 °C while keeping oscillation frequency constant, the duty cycle of the 10 °C muscle would have to be dramatically reduced from 0.42 to only 0.15 (i.e. the optimal duty cycle for this oscillation frequency). Alternatively, if stimulus duty cycle remained constant, then the oscillation frequency would have to decrease dramatically from 4.5 Hz to approximately 1 Hz (Rome and Swank, 1992). On the basis of these facts, to generate a reasonable power at 10 °C, the fish should swim with a far lower tail-beat frequency, far shorter stimulation durations, and perhaps shift the phase of stimulation so that it precedes muscle shortening by a larger amount.

There is no evidence for compensation of this magnitude, nor was there evidence of any compensatory changes in the *in*

vivo length change and stimulation patterns that would improve power generation at 10 °C. We find evidence that only one of the *in vivo* parameters is *potentially* modified at 10 °C compared with 20 °C; however, this change is far too small to improve power production at low temperatures. While swimming at 50 cm s^{-1}, the fish at 10 °C used a slightly lower tail-beat frequency (4.0 *versus* 4.68 Hz) than at 20 °C. The difference in frequency is only approximately 16 %. Further, this difference is larger than that observed at other swimming speeds. The tail-beat frequencies at 40 cm s^{-1} at 10 °C is only approximately 10 % less than at 20 °C and is not statistically different (Fig. 1A). Also, in our previous studies of scup (Rome et al., 1992a), there was no significant difference in tail-beat frequency with temperature when viewed over a wide range of speeds. Even if the difference in tail-beat frequency with temperature observed at 50 cm s^{-1} (this study) was general, it is too small to lead to significant alterations in power output. As noted above, to obtain optimal power output with a duty cycle of 0.4–0.5, the tail-beat frequency would have to decrease by a far greater amount (to approximately 1 Hz), which it clearly does not.

In general, we found that, although EMG duty cycle decreased with swimming speed (Fig. 6), it was independent of temperature and, therefore, there was no compensation for temperature. We did observe that in most cases the value for the stimulation duty cycle was slightly shorter when measured using the rectification-derivative protocol than when measuring the raw recordings manually (compare Fig. 4A with Fig. 6). It should be recognized that analyses of EMG recordings are always somewhat arbitrary: a sensitivity analysis in Rome et al. (1999) demonstrates, however, that the shorter durations determined by computer result in very little change in power output and, thus, do not alter the general conclusions.

In general, the EMG phase was statistically independent of speed and also independent of temperature (Fig. 4C). Thus, there was no physiologically important compensation for temperature. Except for some of the EMG phase data at 50 cm s^{-1} at 20 °C, phase for a given longitudinal position did not vary with swimming speed or temperature (Fig. 4C).

The EMG phase data at 50 cm s^{-1} at 20 °C appeared to diverge from this relationship. At 50 cm s^{-1}, the phase values of the ANT-1 and ANT-2 positions appear to be less negative at 20 °C than at 10 °C. Thus, relative to 20 °C, the 10 °C phase values appeared to be shifted to more negative values. These differences, however, do not represent a compensatory response; rather, they are likely to be a result of increased measurement error and perhaps a difference in swimming style at these speeds. These differences in phase, even if real, cannot be compensatory. As previously mentioned, very large changes in stimulation duty cycle would be required for significant increases in power output. If the stimulation duty cycle is not markedly reduced, the results of Rome and Swank (1992) suggest that muscle generates little net power, *no matter how the phase is adjusted*. In Rome et al. (1999), we show that this is precisely the case. Neither the ANT-1 or ANT-2 muscles generate any power at this speed at 10 °C; hence, there has been no compensation.

Why might some of the phase results from fish at 20 °C at this speed diverge from other data? First, in this group of fish, 50 cm s^{-1} was the approximate speed at 20 °C at which fish went through a gait transition between red muscle burst-and-coast swimming (with some reliance on their pectoral fins) to steady, purely caudal fin swimming. As this speed was easily maintained by these fish and relatively little power is generated at the anterior regions because of the low strain (see Rome et al., 1999), the anterior muscle might still be operating under a transitory gait and, hence, a large variability in the phase might result. Second, measurement errors were largest at this speed, particularly in the anterior region of the fish. The muscle strains were very small, and the EMG amplitudes on average were very low at this speed and temperature. Thus, the determination of phase, which depends on determining the time corresponding to maximum muscle length and the timing of the onset of the EMGs, is subject to more experimental error at this position and speed.

In short, although large compensatory changes in tail-beat frequency and stimulus duty cycle could, in theory, enable the red muscle to generate greater mechanical power at 10 °C, these changes do not occur in scup. One interpretation is that the central pattern generator in fish is not sufficiently flexible to alter the stimulation duty cycles and phases in response to acute exposures to different temperatures. The stimulation duty cycle appears to be essentially independent of oscillation frequency and to depend mostly on position along the length of the fish. Alternatively, some presently underappreciated aspects of power generation and force transmission in the fish as a whole might preclude reducing the stimulus duty cycle at low temperatures.

Having obtained accurate measurements of the *in vivo* length change and stimulation pattern, in the following report (Rome et al., 1999), we drive muscles under their *in vivo* length change and stimulation pattern to determine the effects of temperature, speed and longitudinal position on power generation in the swimming fish. We also introduce sensitivity analysis to determine how sensitive our results are to errors or uncertainties in these parameters. Finally, we integrate the information to provide a more accurate assessment of temperature effects on muscle function and how fish swim at different temperatures

We dedicate this series of papers to the memory of Frank Carey. Frank was a long-time mentor, friend and inspiration who sparked in L.C.R. a career-long interest in temperature, muscle and fish swimming. He organized our stay at the Woods Hole Oceanographic Institution and provided logistical support for this work. The authors also thank M. Grosenbaugh for advice on data analysis and helping to organize our stay, D. Leavitt, B. Lancaster and B. Tripp for facilitating our work at the Coastal Research Center, M. Moore and B. Woodin for helping us find and maintain scup and F. Thurburg of the Bureau of Marine Fisheries for lending us the water treadmill. We thank Dave Corda for helping

swim the fish and analyze the films and Jun-uk Kim for performing the quantitative EMG analysis. We also thank Dr David Coughlin for performing several analyses used in this manuscript and Dr Iain Young for critically reviewing the manuscripts. Supported by NIH AR38404, NIH AR46125, NSF IBN-9514383 and the University of Pennsylvania Research Foundation.

References

Altringham, J. D., Wardle, C. S. and Smith, C. I. (1993). Myotomal muscle function at different locations in the body of a swimming fish. *J. Exp. Biol.* **182**, 191–206.

Coughlin, D. J., Valdes, L. and Rome, L. C. (1996). Muscle length changes during fish swimming: a comparison of sonomicrometry and anatomical-high speed ciné techniques. *J. Exp. Biol.* **199**, 459–463.

Davies, M. L. and Johnston, I. A. (1995). Muscle fibers in rostral and caudal myotomes of the atlantic cod (*Gadus morhua* L.) have different mechanical properties. *Physiol. Zool.* **68**, 673–697.

Hammond, L., Altringham, J. D. and Wardle, C. S. (1998). Myotomal slow muscle function of rainbow trout *Oncorhynchus mykiss* during steady swimming. *J. Exp. Biol.* **201**, 1659–1671.

Jayne, B. C. and Lauder, G. V. (1995a). Speed effects on midline kinematics during steady undulatory swimming of largemouth bass, *Micropterus salmoides*. *J. Exp. Biol.* **198**, 585–602.

Jayne, B. C. and Lauder, G. V. (1995b). Red muscle motor patterns during steady swimming in largemouth bass: effects of speed and correlations with axial kinematics. *J. Exp. Biol.* **198**, 1575–1587.

Johnson, T. P. and Johnston, I. A. (1991). Power output of fish muscle fibres performing oscillatory work: effects of acute and seasonal temperature change. *J. Exp. Biol.* **157**, 409–423.

Josephson, R. K. (1993). Contraction dynamics and power output of skeletal muscle. *Annu. Rev. Physiol.* **55**, 527–546.

Marsh, R. L. (1990). Deactivation rate and shortening velocity as determinants of contractile frequency. *Am. J. Physiol.* **259**, R223–R230.

Olson, J. M. and Marsh, R. L. (1993). Contractile properties of the striated adductor muscle in the bay scallop *Argopecten irradians* at several temperatures. *J. Exp. Biol.* **176**, 175–193.

Rall, J. A. and Woledge, R. C. (1990). Influence of temperature on mechanics and energetics of muscle contraction. *Am. J. Physiol.* **259**, R197–R203.

Rome, L. C. (1982). The energetic cost of running with different muscle temperatures in savannah monitor lizards. *J. Exp. Biol.* **97**, 411–426.

Rome, L. C. (1986). The influence of temperature on muscle and locomotory performance. In *Living in the Cold: Physiological and Biochemical Adaptations* (ed. H. C. Heller, H. J. Musacchia and L. C. H. Wang), pp. 485–495. New York: Elsevier.

Rome, L. C. (1990). The influence of temperature on muscle recruitment and function *in vivo*. *Am. J. Physiol.* **259**, R210–R222.

Rome, L. C. (1995). A device for synchronizing physiological data to cine film. *J. Biomech.* **28**, 333–338.

Rome, L. C., Choi, I., Lutz, G. and Sosnicki, A. A. (1992a). The influence of temperature on muscle function in fast swimming scup. I. Shortening velocity and muscle recruitment during swimming. *J. Exp. Biol.* **163**, 259–279.

Rome, L. C., Funke, R. P. and Alexander, R. McN. (1990). The influence of temperature on muscle velocity and sustained performance in swimming carp. *J. Exp. Biol.* **154**, 163–178.

Rome, L. C., Loughna, P. T. and Goldspink, G. (1984). Muscle fiber recruitment as a function of swim speed and muscle temperature in carp. *Am. J. Physiol.* **247**, R272–R279.

Rome, L. C. and Sosnicki, A. A. (1990). The influence of temperature on mechanics of red muscle in carp. *J. Physiol., Lond.* **427**, 151–169.

Rome, L. C. and Sosnicki, A. A. (1991). Myofilament overlap in swimming carp. II. Sarcomere length changes during swimming. *Am. J. Physiol.* **260**, C289–C296.

Rome, L. C., Sosnicki, A. A. and Choi, I. (1992b). The influence of temperature on muscle function in the fast swimming scup. II. The mechanics of red muscle. *J. Exp. Biol.* **163**, 281–295.

Rome, L. C. and Swank, D. (1992). The influence of temperature on power output of scup red muscle during cyclical length changes. *J. Exp. Biol.* **171**, 261–281.

Rome, L. C., Swank, D. and Corda, D. (1993). How fish power swimming. *Science* **261**, 340–343.

Rome, L. C., Swank, D. and Coughlin, D. (2000). The influence of temperature on power production during swimming. II. Mechanics of red muscle fibres *in vivo*. *J. Exp. Biol.* **203**, 333–345.

Swank, D., Zhang, G. and Rome, L. C. (1997). Contraction kinetics of red muscle in scup: mechanism for variation in relaxation rate. *J. Exp. Biol.* **200**, 1297–1307.

Swoap, S. J., Johnson, T. P., Josephson, R. K. and Bennett, A. F. (1993). Temperature, muscle power output and limitations on burst locomotory performance of the lizard *Dipsosaurus dorsalis*. *J. Exp. Biol.* **174**, 185–197.

van Leeuwen, J. L., Lankheet, M. J. M., Akster, H. A. and Osse, J. W. M. (1990). Function of red axial muscle of carp (*Cyprinus carpio* L.): recruitment and normalised power output during swimming in different modes. *J. Zool., Lond.* **220**, 123–145.

Wardle, C. S. and Videler, J. J. (1993). The timing of electromyograms in the lateral myotomes of mackerel and saithe at different swimming speeds. *J. Fish Biol.* **42**, 347–359.

Wardle, C. S., Videler, J. J. and Altringham, J. D. (1995). Tuning in to fish swimming waves: body form, swimming mode and muscle function. *J. Exp. Biol.* **198**, 1629–1636.

Williams, T. L., Grillner, S., Smoljaninov, V. V., Wallén, P., Kashin, S. and Rossignol, S. (1989). Locomotion in lamprey and trout: the relative timing of activation and movement. *J. Exp. Biol.* **143**, 559–566.

Woledge, R. C. (1992). Relaxation as a determinant of the locomotory role of muscle. *SEB Annual Meeting* (Abstract).